SUPPLEMENTARY INFORMATION

Tunable and Compartmentalized Multimaterial Bioprinting for Complex Living Tissue Constructs

*Shabir Hassan[1], Eduardo Gomez Reyes[1,2], Eduardo Enciso-Martinez[1,2], Kun Shi[1,3], Jorge Gonzalez Campos[1,2], Oscar Yael Perez Soria[1,2], Eder Luna-Cerón[1,2], Myung Chul Lee[1], Isaac Garcia Reyes[1,2], Joshua Steakelum[1,5], Haziq Jeelani[4], Luis Enrique García-Rivera[1,2], Minsung Cho[6], Stephanie Sanchez Cortes[1,2], Tom Kamperman[1,7], Haihang Wang[1], Jeroen Leijten[7], Lance Fiondella[5], Su Ryon Shin[1]**

[1]Division of Engineering in Medicine, Department of Medicine, Harvard Medical School, and Brigham and Women's Hospital, Cambridge, MA, 02139, USA.

[2]Tecnológico de Monterrey at Monterrey, Monterrey, Nuevo León, CP 64849, Mexico

[3]State Key Laboratory of Biotherapy and Cancer Center, West China Hospital, Sichuan University and Collaborative Innovation Center of Biotherapy, Chengdu, 610041, PR China

[4] Institute of Electrical and Electronics Engineers (IEEE), New York, 10016, USA.

[5] Department of Electrical and Computer Engineering, University of Massachusetts, Dartmouth MA 02747, USA

[6] AltrixBio inc., Cambridge, MA 02139, USA

[7] Department of Developmental Bioengineering, Faculty of Science and Technology, TechMed Centre, University Twente, Enschede, 7522 NB, Netherlands

*Correspondence at: sshin4@bwh.harvard.edu; shin.lotus@gmail.com

Contents

Supplementary Figures

Supplementary Movies

Supplementary Tables

Supplementary Table S1 | Comparison of different multimaterial bioprinter speeds from the literature.

Supplementary Figures

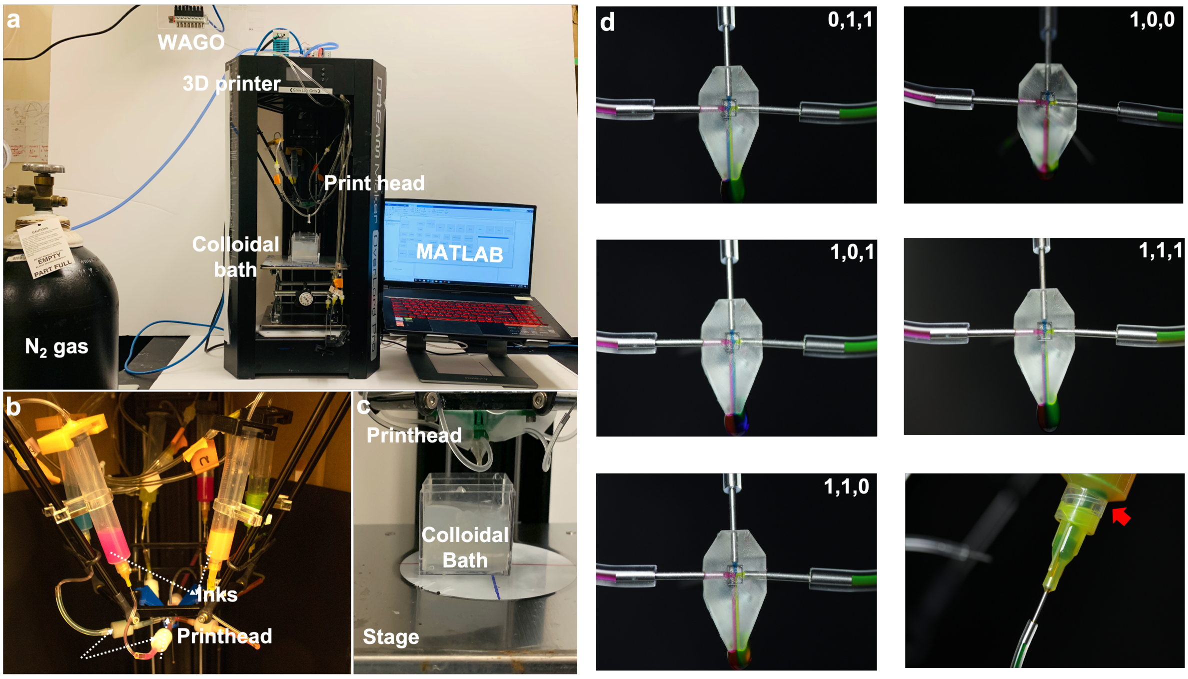

Figure S1 | M^3 system. a, Photograph showing different components of the printing system. **b,** Close-up of different ink syringes (6 in this case) feeding into the single nozzle printhead via check valves. **c,** colloidal bath sitting on a stage where printing happens. and **d,** Effect of check valve on ink mixing when opened (1) or closed (0) for Red (R), Green (G), and Blue (B), respectively. Binary codes are sequentially for RGB inks.

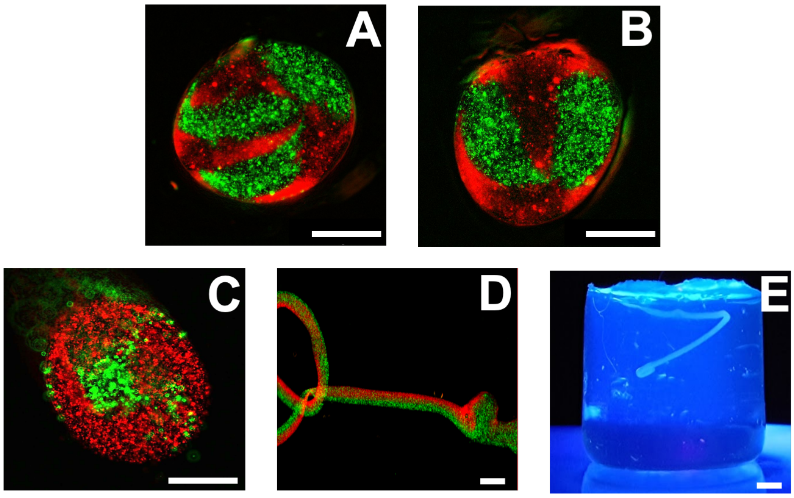

Figure S2 | Unique printing shapes from M^3. **a**, basket shape, **b**, insect eye, **c**, solid donut with green core and red shell, **d**, knot, **e**, serpentine shapes, respectively. Scale bars=500 µm.

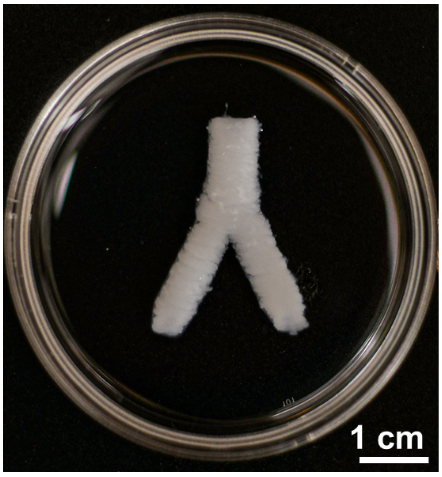

Figure S3 | Y-shaped bioprinted branched vessel in high resolution.

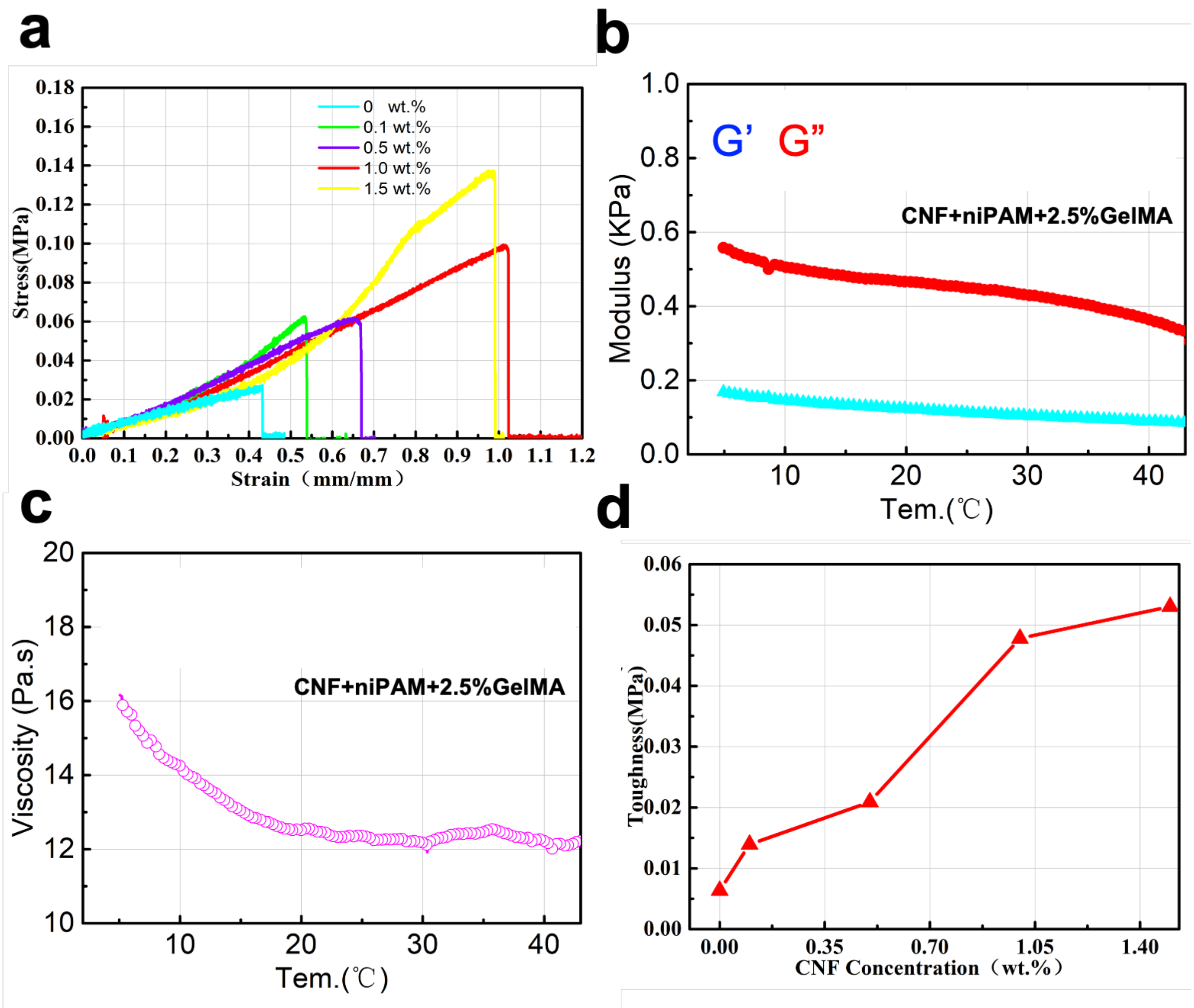

Figure S4 | Mechanical and rheological properties of CNF, NIPAM, and GelMA composite bioink. a, Stress strain curves of composite inks at different wt% of CNF. **b**, Storage (G') and loss (G") moduli of the composite inks. The higher G' values than the G" values correspond to high fidelity prints from the ink. **c**, Effect on viscosity as a function of temperature. The inks flow efficiently at and above the temperatures of 20 °C, the temperature. **d**, Graph shows the effect of increasing CNF on the toughness of the ink.

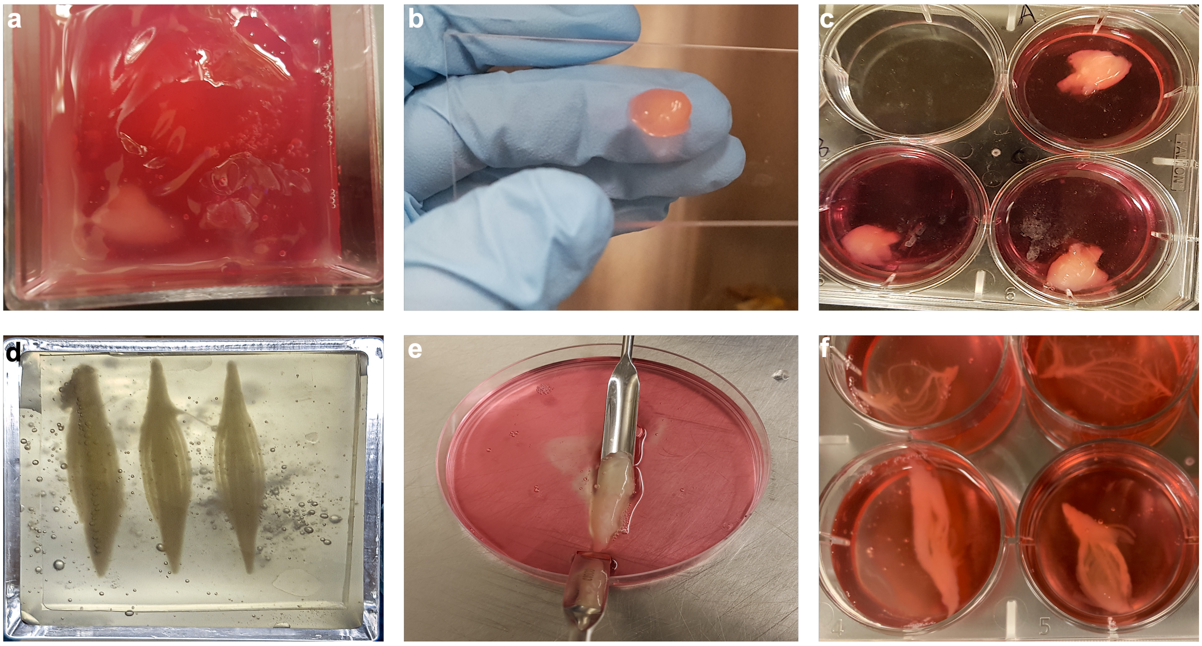

Figure S5 | Bioprinted constructs of liver-like and muscle fiber mimic constructs. a-c) Printed liver-like construct in a GCG bath before taking out for culturing, after washing off GCG, and in culture media, respectively. **d**, Several muscle fiber mimic constructs can be printed at the same time in a single support bath. **e**, Individual fibrils in the muscle fiber can be seen clearly; **f**, GCG washed off from the printed muscle fiber before being put in the incubator for cell culture in **e**.

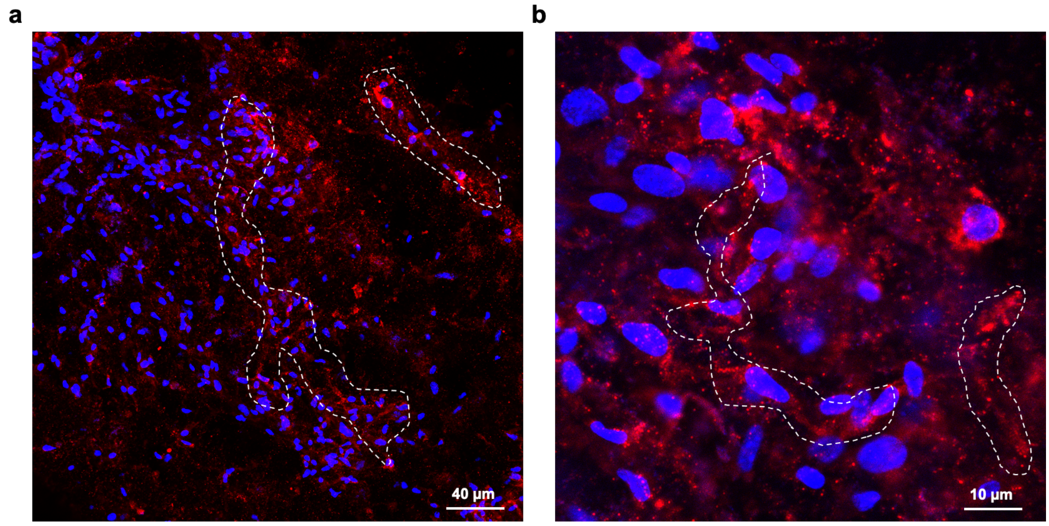

Figure S6: CD31 immunostaining of bioprinted muscle fiber mimic scaffold. The figures show the areas of possible initiation of neovascularization on account of a stronger CD31 signal at different magnifications (a) and (b).

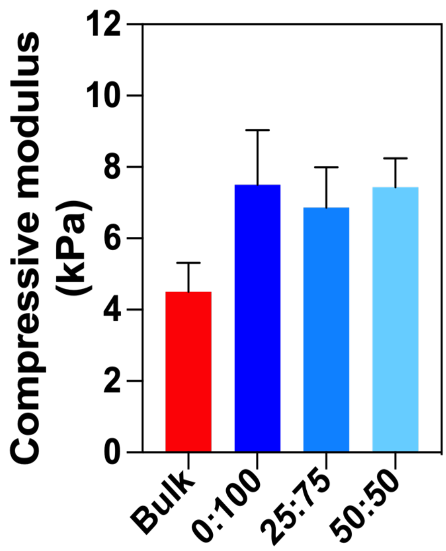

Figure S7 | Compressive modulus of GCGs. Compressive moduli of GCGs with different gelatin: GelMA ratio (gelatin: GelMA = 0:100, 25: 75, and 50:50).

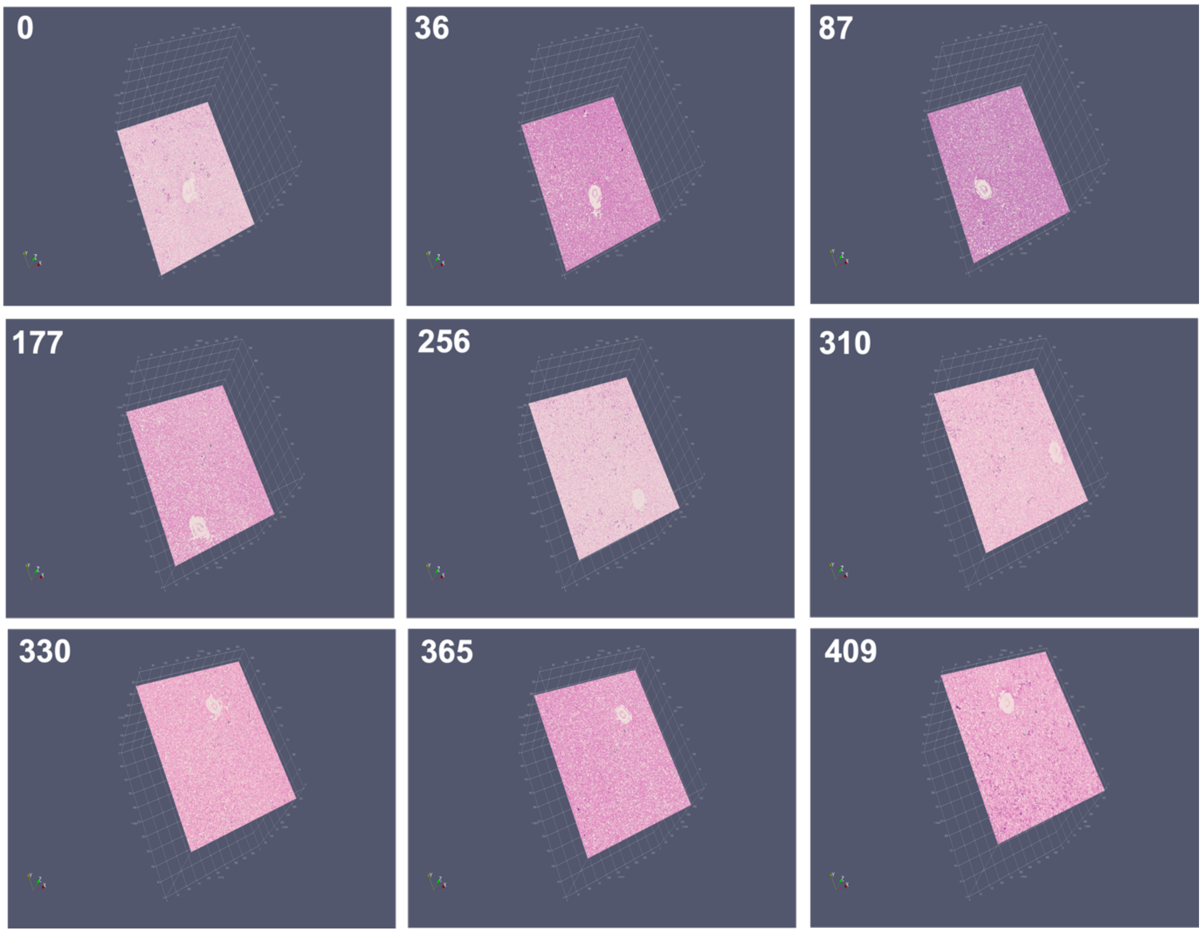

Figure S8 | Reconstruction slices of the 3D volumetric rendition of the in vivo explant. Numbers on the images depict the slice number of the snapshots reconstructed by SIRT for the volume rendition.

Supplementary Movies

Movie S1 | Pressure valve gating. Simulation showing controlled dispensation of 7 different inks through the printhead.

Movie S2 | Printing in absence of check valves. Ink mixing due to backflow pressure in absence of check valves. Scale bar 5 mm.

Movie S3 | Printing in presence of check valves and fast switching. Inks can flow individually without backflow pressure and hence no intermixing in presence of check valves. Check valves in this case were switched at 5Hz. Scale bar 5 mm.

Movie S4 | Choice of bioink mixing. Ink extrusions can be controlled with precision. Shown in the video is co-flow of RGB, R, B, G, RB, RG, and BG inks in a sequential manner. (Video played at 4X speed) RGB represent inks with red, green, and blue color, respectively. Scale bar 5 mm.

Movie S5 | Multimaterial bioprinting at high speed. Demonstration of bioprinting with two inks where check valves are switched at a frequency of 4Hz. Scale bar 5 mm.

Movie S6 | Simulation of 2 inks mixing and extrusion

Movie S7 | Simulation of 4 inks mixing and extrusion

Movie S8 | Simulation of 6 inks mixing and extrusion

Movie S9 | Simulation of 7 inks mixing for core-shell geometry

Movie S10 | Simulation of 7 inks mixing for donut shaped geometry

Movie S11 | Perfusion across a hollow linear vessel

Movie S12 | Bioprinting of liver construct. (Video played at 8X speed)**.**

Movie S13 | Bioprinting of a skeletal muscle. (Video played at 8X speed)

Movie S14 | Volumetric reconstruction of the bioprinted spiral 7 days post implantation (Video played at 4X speed)

Supplementary Table S1

Comparison of different multimaterial bioprinter speeds from the literature

Bioprinter Feature	Mode	Maximum Speed	Authors	Reference
Multimaterial 3D bioprinter	Single nozzle multimaterial	10 m/s	Kolesky D B et al	1
Rapid continuous multimaterial extrusion bioprinting	Multinozzle (Co-axial) multimaterial	~ 10mm/s	Liu W et al	2
6 Degree of freedom bioprinter with pressure pump	Multinozzle (Co-axial) multimaterial	20 mm/s	Khan Z et al	3
3D biofactory	Single nozzle multimaterial	0.4 mm/s	Avila-Ramirez A et al	4
A hybrid bioprinting approach for scale-up tissue fabrication	Multi-arm hybrid bioprinter	14 mm/s	Yu Y et al	5
Intra-volumetric multimaterial	Single nozzle multimaterial	~ 25 mm/s	Hassan S et al	This manuscript

References

1. Kolesky, D. B.; Truby, R. L.; Gladman, A. S.; Busbee, T. A.; Homan, K. A.; Lewis, J. A., 3D Bioprinting of Vascularized, Heterogeneous Cell-Laden Tissue Constructs. *Advanced Materials* **2014,** *26* (19), 3124-3130.
2. Liu, W.; Zhang, Y. S.; Heinrich, M. A.; De Ferrari, F.; Jang, H. L.; Bakht, S. M.; Alvarez, M. M.; Yang, J.; Li, Y. C.; Trujillo-de Santiago, G.; Miri, A. K.; Zhu, K.; Khoshakhlagh, P.; Prakash, G.; Cheng, H.; Guan, X.; Zhong, Z.; Ju, J.; Zhu, G. H.; Jin, X.; Shin, S. R.; Dokmeci, M. R.; Khademhosseini, A., Rapid Continuous Multimaterial Extrusion Bioprinting. *Adv Mater* **2017,** *29* (3).
3. Khan, Z.; Kahin, K.; Rauf, S.; Ramirez-Calderon, G.; Papagiannis, N.; Abdulmajid, M.; Hauser, C. A. E., Optimization of a 3D bioprinting process using ultrashort peptide bioinks. *Int J Bioprint* **2018,** *5* (1), 173-173.
4. Avila-Ramirez, A.; Catzim-Ríos, K.; Guerrero-Beltrán, C. E.; Ramírez-Cedillo, E.; Ortega-Lara, W., Reinforcement of Alginate-Gelatin Hydrogels with Bioceramics for Biomedical Applications: A Comparative Study. *Gels* **2021,** *7* (4), 184.
5. Yu, Y.; Zhang, Y.; Ozbolat, I. T., A Hybrid Bioprinting Approach for Scale-Up Tissue Fabrication. *Journal of Manufacturing Science and Engineering* **2014,** *136* (6).